# Decentralized Voltage Control of AC Microgrids with Constant Power Loads using Control Barrier Functions

Grigoris Michos, and George C. Konstantopoulos

Abstract—This paper proposes a novel nonlinear decentralized voltage controller for constrained regulation of meshed AC Microgrid networks with high penetration of constant power loads. Perceiving the load demand as an unknown disturbance, the network model is reformulated in a cascaded structure composed of a nominal, *i.e.* uncertainty-free, and an error subsystem. The latter captures the distance between the true and the nominal state trajectories, for which we prove boundedness via a suitable control barrier function. Under sufficient conditions, we prove asymptotic stability of the cascaded dynamics with respect to an equilibrium set and also provide an estimate of the region of attraction. In addition, it is rigorously shown that the proposed nonlinear control law also enforces constrained regulation around a rated voltage value, without the need of saturation devices. The operation of the closed-loop system is illustrated in a simulation scenario, demonstrating bounded operation and convergence to a neighbourhood of the desired reference vector.

Index Terms—Nonlinear Systems, Electric Power Networks, Robust Control, Stability, Constant Power Loads

## I. LITERATURE REVIEW

The modern power grid is undergoing a transformative evolution from a traditionally centralized infrastructure to a decentralized entity. This shift is largely driven by the growing penetration of renewable energy sources (RES), which are increasingly being deployed in distributed configurations across both communities and isolated areas. The concept of Microgrid has emerged, in order to facilitate the decentralized regulation of the various distributed generation (DG) units and enable their integration with the main power grid. However, the reduced presence of synchronous generators (SGs) and rotational kinetic energy in the power grid has a negative effect on the total system inertia, increasing its susceptibility to surges in power demand and faults [1].

A Microgrid has the ability to operate both in grid-connected and islanded mode. In the former, the local converters operate in a grid-following mode, where the voltage levels are dictated by a strong grid. On the other hand, in islanded mode both the voltage and the frequency are regulated by the so-called grid-forming converters. This case is particularly challenging due to the lack of SGs and their ability to store large amounts of energy within their rotational movement. Traditionally, voltage control for islanded Microgrid is achieved

This work was performed within the TARGET-X framework, a project funded by the Smart Networks and Services Joint Undertaking (SNS JU) under Horizon Europe (funding number 101096614). The authors are with the Department of Electrical and Computer Engineering, University of Patras, Rion 26504, Greece. (e-mail: grmichos@upatras.gr, g.konstantopoulos@ece.upatras.gr)

in an indirect fashion, where the employed strategy focuses on adjusting the reference points and inner cascaded loops are utilized to track these points. The prevalent strategy in the literature is the droop control, where the state references are computed by mimicking the droop curves of a SG, where the inner loops are often regulated via linear propotional-integral controllers [2]. Other control strategies such as the Virtual Sychnronous Machine control involve emulation of the SG [3] that can provide reliable grid support but require careful tuning of the inner loops to avoid instability. In an effort to achieve stronger stability guarantees compared to the aforementioned strategies, the dispatchable virtual oscillator approaches were proposed, see for example [4]. Therein, it is shown that for

some network topologies it is indeed possible to achieve (semi)

global asymptotic stability certificates.

Designing controllers that achieve stable closed-loop performance is still an open problem in the literature, especially when one considers the full complexity of the modern power grid. There are two main categories in the literature that investigate the stability of grid-forming converters, and by extension islanded Microgrid configurations. The majority of the proposed studies fall within the first, namely studies that numerically validate the stability certificates of the proposed closed-loop system [5]-[9]. The second category involves analytic approaches that either study the system behaviour locally in a neighbourhood of an operating point [10]–[13] or attempt to achieve global results in a large-signal sense [14]–[18]. However, to the best of our knowledge, there exist a limited number of studies investigating constant power demand in the network. Contrary to the literature of DC Microgrids, where the concept of constant power loads (CPLs) has being gaining increasing attention over the past few years, see for example [19]-[22], in the case of AC Microgrid systems there is a large gap of control-theoretic studies considering the connection of tightly controlled power converters or rectifiers to the AC network. In this cases, the AC side is required to meet a constant power demand, which, similarly to the case of a DC Microgrid, can significantly degrade the system stability [23], [24]. Numerical or local approximation approaches have been proposed in [25]-[27], however these require the knowledge of the network parameters and do not consider the nonlinear characteristics of the system. The system dynamic model was considered in [23] but the stability certificates are only numerically investigated. An infinity-norm criterion was established in [28], but is limited in providing results for a single inverter feeding a constant power load, while the

analysis also omits the system nonlinearities. Overall, the topic of AC Microgrids with large penetration of constant power loads is largely unexplored and, to the best of our knowledge, no analytic results have been established that provide system stability in a rigorous fashion.

A second important topic is the strict voltage limitation within a desired operating region. Considering the low system inertia and the lack of sufficient energy storage capacity of inverter-based networks, the system becomes vulnerable to power surges and voltage drops. Generally, the task of constraint satisfaction is achieved by a supervisory controller, which only addresses steady-state performance [29], [30]. A few studies have proposed controller schemes that incorporate this requirement in the primary control level; the authors of [31] propose a model-based voltage controller for AC Microgrids that tracks reference points provided by solving a constrained optimization problem. An optimization-based controller was also provided in [32], where a model-predictive controller established constrained voltage regulation and robustness with respect to system disturbances. However, the former study is limited in investigating bounds on the steadystate values, while the latter requires knowledge of the network parameters. In addition, both approaches impose a large computational load, especially in the case of AC Microgrids that operate in fast time scales. In [33], a nonlinear controller enforces an upper bound on the voltage trajectory, however the study only considers purely passive networks.

The concept of control barrier functions (CBFs) has risen in the literature of control, in an effort to enforce the system states to operate within a "safe" region [34], [35]. The main benefit of this approach is that it is possible to establish set invariance under the system trajectories without requiring invariance of each sublevel set, i.e. a necessary property of Lyapunov-based approaches. Recently, CBFs have begun gaining interest in the literature of power systems. A CBF-based supervisory controller was proposed in [36] for inverter-based networks. The authors of [37] propose a CBF approach to ensure network resilience and voltage restoration to a "safe" region. The regulation of inverter-based Microgrids is studied in [38], where the proposed controller utilizes CBFs to enforce voltage constraints both during transient and steady state performance. While a promising approach, the application of CBFs on AC microgrids is largely unexplored, with many studies focusing on the DC counterpart. Nevertheless, CBFs can play a crucial role in designing stabilizing controllers for AC Microgrid networks that are required to satisfy constant power load demand, where the dynamics are no longer Lipschitz continuous around the origin.

This article aims to fill the gap identified in the literature, by proposing a nonlinear voltage control law that stabilizes the network under CPL demand, and enforces constrained operation around a rated voltage value. Specifically, we perceive the CPL demand as a system disturbance and propose a tube-control approach, where the original dynamics are expressed by a nominal, *i.e.* disturbance-free, and an error state. Then, we employ a CBF to rigorously ensure that the distance between the true and the nominal voltage trajectories, *i.e.* the tube width, does not grow unbounded and is contained

within a robustly positive invariant (RPI) set. Furthermore, we show asymptotic stability and constrained operation of the network system under sufficient conditions on the magnitude of the controller parameters. As opposed to [29]–[32], [39], [40] the proposed control design enforces voltage constrains by directly manipulating the closed-loop system dynamics, without the need of employing optimization-based techniques that require both knowledge of the network parameters and impose a large computational load. This way, we are able to guarantee satisfaction of the voltage constraints both during transient and steady state performance. In addition, contrary to [33], we prove that the proposed approach achieves the aforementioned objectives, despite the presence of non-passive elements in the network. Furthermore, regarding the literature on AC Microgrids with CPLs [23], [25]-[28], we provide for the first time analytic stability guarantees using Lyapunov theory and an estimate for the region of attraction for the closed-loop system equilibrium set.

This article, extends the previous work of the authors in [41] in two ways; firstly, we deduce explicit conditions with respect to a desired maximum deviation between the true voltage trajectory from the nominal. This is opposed to the more conservative approach in [41], where the RPI set has a fixed size and is nonconvex. Secondly, this study proposes a unified control strategy, in the sense that we also adopt a nonlinear control law for the nominal dynamics. The structure of the proposed nonlinear control law is exploited to analytically establish constraint satisfaction and asymptotic stability of the true voltage dynamics with respect to an admissible equilibrium set.

The structure of the article is organized as follows. Sections II and III derive the system model using a graph representation of the Microgrid network and specify the control objectives for the control design. Then, Section IV provides the first major result, by formulating sufficient conditions, under which the proposed set is RPI. The second main result is established in Section V, where we prove boundedness of the nominal trajectory in a desired constraint set and asymptotic stability of the nodal nominal setpoints. Then, the desired stability certificates of the cascaded system are proven in Section VI. Section VII includes an illustrative example on the operation of the closed-loop system under the proposed control law, demonstrating the strong theoretic properties established from the previous Sections. Finally, Section VIII provides concluding remarks and future research directions.

## A. Notation

For a vector  $a \in \mathbb{R}^n$ , the  $s^{\text{th}}$  self-Hadamard product is denoted by  $a^s$ , while  $\|a\|$  denotes the euclidean norm unless otherwise specified. The notation [a] denotes a diagonal matrix with diagonal elements  $[a]_{ii} = a_i$ . The  $n \times n$  zero and identity matrices are denoted as  $0_n$  and  $I_n$  respectively. The Minkowski sum  $A \oplus B$  of two sets  $A \in \mathbb{R}^n$  and  $B \in \mathbb{R}^n$  is defined as  $A \oplus B := \{a+b\colon a \in A, b \in B\}$ . Furthermore, we define the matrix  $J_{2n}$  as

$$J_{2n} = \begin{bmatrix} 0_n & I_n \\ -I_n & 0_n \end{bmatrix}.$$

Consider the nonlinear system  $f \colon \mathbb{R}^n \to \mathbb{R}^n$  given by

$$\dot{x} = f(x). \tag{1}$$

**Theorem 1** (Bony-Brezis [42]). Consider the nonlinear dynamics in (1) and a closed subset  $S \subset \mathbb{R}^n$ . Let the following two conditions hold,

- 1)  $|f(x) f(y)| \le K|x y|$ , for some  $K \in \mathbb{R}$  and all  $x, y \in \mathcal{S}$ .
- 2)  $\langle f, \nu \rangle \leq 0$ , where  $\nu \in \mathbb{R}^n$  is the normal vector on S. Then, the set S is positive invariant under the solution of the dynamics (1).

**Definition 1.** Consider the nonlinear dynamics in (1), a continuously differentiable function  $b \colon \mathbb{R}^n \to \mathbb{R}$  and a set S defined by

$$S := \left\{ x \in \mathbb{R}^n \colon \ b(x) \ge 0 \right\} \tag{2a}$$

$$\partial \mathcal{S} := \left\{ x \in \mathbb{R}^n \colon \ b(x) = 0 \right\} \tag{2b}$$

The function  $b(\cdot)$  is called a control barrier function, if for any  $x \in \mathcal{S}$ 

$$\inf_{x \in \partial \mathcal{S}} \left\{ \mathfrak{L}_f b(x) \right\} \ge 0 \tag{3}$$

where  $\mathfrak{L}_f$  is the Lie derivative defined by  $\mathfrak{L}_f \coloneqq \frac{\partial b(x)}{\partial x} f(x)$ .

## II. PRELIMINARIES

In this paper we investigate the problem of a Microgrid network consisting of n DG units. Each ith unit, with  $i \in \mathcal{M} \coloneqq \{1,2,3,\ldots,n\}$ , is interfaced with the network via 3-phase power inverters, local nonlinear loads and primarily inductive lines. This facilitates an analysis, where the Microgrid is viewed as an undirected graph  $\mathcal{G} = (\mathcal{M}, \mathcal{E})$ , where  $\mathcal{M} \in \mathbb{R}^m$  is the set of nodes and  $\mathcal{E} \in \mathcal{M} \times \mathcal{M}$  is the set of edges, characterizing the connections between the nodes with e = (i,j) for  $i,j \in \mathcal{M}$ . We assign a unique index to each edge  $e \in \mathcal{E} := \{1,2,\ldots,m\}$ . Then, the topology of the network is described by the oriented incidence matrix  $B \in \mathbb{R}^{m \times n}$  defined as,

$$B_{\epsilon i} = \begin{cases} 1, & \text{if the edge is } (i,j) \text{ for some } j \\ -1, & \text{if the edge is } (j,i) \text{ for some } j \\ 0, & \text{otherwise} \end{cases}$$
 (4)

This allows us to assign an arbitrary direction for the network line currents.

We consider that each inverter is interfaced to the network by LC-filters, while the loads are modelled as constant power loads connected in parallel to the inverter output filter capacitor. Furthermore, in order to simplify the analysis, it is assumed that the injected current dynamics are operating in a sufficiently higher time-scale compared to the capacitor voltage, such that the injected current can be considered constant in the mathematical analysis of the capacitor voltage dynamic model. This is a common assumption in the literature dating back to [43]. In essence this allows us to consider the inverters as a controllable current source connected in parallel to an output capacitor. Then, similarly to [44], [45], implementing the Kirchhoff laws yields the system model

in a d-q frame rotating in a common global frequency  $\omega_g$ , that describes the dynamic behaviour of each node and the interactions with the network currents

$$C_{i}\dot{v}_{d,i} = I_{inj,id} + \omega_{g}C_{i}v_{q,i} - B_{i}^{\top}I_{E,d} - g_{d,i}(v_{d,i}, v_{q,i}, P_{i}, Q_{i})$$
 (5a)

$$C_{i}\dot{v}_{q,i} = I_{inj,iq} - \omega_{g}C_{i}v_{d,i} - B_{i}^{\top}I_{E,q} - g_{a,i}(v_{d,i}, v_{g,i}, P_{i}, Q_{i})$$
 (5b)

$$L_E \dot{I}_{E,d} = -r_E I_{E,d} + \omega_a L_E I_{\varepsilon,a} + B v_d \tag{5c}$$

$$L_E \dot{I}_{E,q} = -r_E I_{E,q} - \omega_g L_E I_{\varepsilon,d} + B v_q \tag{5d}$$

In the above,  $C_i \in \mathbb{R}_{>0}$  is the nodal capacitance of each inverter output filter,  $L_E \in \mathbb{R}^{m \times n}$  is a diagonal matrix collecting the inductance of each line with index  $\epsilon \in E$  and a diagonal matrix  $r_E \in \mathbb{R}^{m \times m}$  collects the line resistances. The pair  $(v, I_E)$  represents the system states, where  $v = [v_d \ v_q]^\top \in \mathbb{R}^{2n}$  collects the voltages of the each node output capacitor and  $I_E = [I_{E,d} \ I_{E,q}]^\top \in \mathbb{R}^{2m}$  are the network line currents. The input to the system are the inverter injected currents  $I_{inj} = [I_{inj,d} \ I_{inj,q}]^\top \in \mathbb{R}^{2n}$ . Finally, the local constant power load demand is characterised by the function  $g_i \colon \mathbb{R}^2 \times \mathbb{R}^2 \times \mathbb{R} \times \mathbb{R} \to \mathbb{R}^2$  given by  $g_i = [g_{d,i} \ g_{q,i}]^\top$ , where

$$g_{d,i}(v_{d,i}, v_{q,i}, P_i, Q_i) = \frac{2}{3} \left( \frac{v_{d,i}}{v_{d,i}^2 + v_{q,i}^2} P_i + \frac{v_{q,i}}{v_{d,i}^2 + v_{q,i}^2} Q_i \right)$$
(6a)

$$g_{q,i}(v_{d,i}, v_{q,i}, P_i, Q_i) = \frac{2}{3} \left( \frac{v_{q,i}}{v_{d,i}^2 + v_{q,i}^2} P_i - \frac{v_{d,i}}{v_{d,i}^2 + v_{q,i}^2} Q_i \right)$$
(6b)

where  $P_i \in \mathbb{R}$ ,  $Q_i \in \mathbb{R}$  are the active and reactive power demand for each ith local load. In this study, the Microgrid is subject to operational constraints on the values obtained in the nodal voltages, i.e. we require  $v_i(t) \in \mathbb{V}_i$  at all times. The following assumption provides common desired properties of the state constraint set, which will be useful in the closed-loop system analysis.

**Assumption 1** (Operational constrains). For all  $i \in \mathcal{M}$ , the nodal voltage constraint set  $\mathbb{V}_i \subset \mathbb{R}^2$  is non-empty and compact. Furthermore, it holds that

$$\mathbb{V} = \prod_{i \in \mathcal{M}} \mathbb{V}_i,$$

where  $V_i := \left\{ v_i \in \mathbb{R}^2 \colon \left\| v_i - v_i^o \right\| \le v_i^{\max} \right\}$ , with  $v_i^o$  a rated voltage and  $v_i^{\max} \ll v_i^o$  a maximum deviation from the rated value.

Following the above assumption, the state constraint is a Cartesian product of each local constraint set, indicating that there exist no coupled constraints in the network.

It is possible to simplify the network dynamic model by considering that the lines operate in a sufficiently larger time constants. This allows the consideration of (5) as a singularly perturbed system operating in two time scales [46]. The simplified model is given by

$$C_{i}\dot{v}_{d,i} = I_{inj,id} + \omega_{g}C_{i}v_{q,i} - \mathcal{L}_{i}^{\top}v_{d} - g_{d,i}(v_{d,i}, v_{q,i}, P_{i}, Q_{i}),$$
(7a)  

$$C_{i}\dot{v}_{q,i} = I_{inj,iq} - \omega_{g}C_{i}v_{d,i} - \mathcal{L}_{i}^{\top}v_{q} - \mathcal{L}_{i}v_{q} - g_{q,i}(v_{d,i}, v_{q,i}, P_{i}, Q_{i})$$
(7b)

where  $\mathcal{L}_i$  is the respective ith column associated with the network Laplacian matrix  $\mathcal{L} \in \mathbb{R}^{n \times n}$ , given by  $\mathcal{L} = B^{\top} \left( -r_E + \omega_g L_E \right)^{-1} B$ . The above structure is a direct result of substituting the equilibrium of the line currents subsystem into the voltage dynamics of the respective local bus.

## III. PROBLEM FORMULATION

## A. Derivation of cascaded system dynamics

In this section we will formally present the investigated problem and formulate the control objectives. First it is noted that the system uncertainty arises from the perturbations of the CPL demand. Let the active and reactive power required by the load be a deviation from some known constant value, *i.e.* 

$$P_i = \bar{P}_i + \delta P_i, \tag{8a}$$

$$Q_i = \bar{Q}_i + \delta Q_i, \tag{8b}$$

where  $\bar{P}_i, \bar{Q}_i \in \mathbb{R}$  are known constant values and  $\delta P_i, \delta Q_i \in \mathbb{R}$  are the unknown deviations. Furthermore, we invoke the following assumption, establishing an upper bound on the power demand deviations.

**Assumption 2.** For all  $i \in \mathcal{M}$ , there exist  $P_{\max,i} \in \mathbb{R}_{>0}$  and  $Q_{\max,i} \in \mathbb{R}_{>0}$  such that,

$$\delta P_i \in \mathbb{W}_{P,i} := \left\{ \delta P_i \in \mathbb{R} \colon \| \delta P_i \| \le \delta P_{\max,i} \right\},$$
  
$$\delta Q_i \in \mathbb{W}_{Q,i} := \left\{ \delta Q_i \in \mathbb{R} \colon \| \delta Q_i \| \le \delta Q_{\max,i} \right\}$$

Following this formulation of the disturbance, it is possible to restructure the dynamical model (7) to a pair of a nominal state, perceiving a constant disturbance, and an error describing the difference between the nominal and the true dynamics. To achieve this, we define a error state  $e_i = [e_{d,i} \ e_{q,i}]^{\top}$  as

$$e_i = v_i - z_i \tag{9}$$

where  $z_i \in \mathbb{R}^2$  is a nominal state associated to a nominal subsystem with dynamic model given by

$$C_i \dot{z}_i = \bar{I}_{inj,i} + J_2 \omega_g C_i z_i - \mathcal{L}_i^{\top} z - g_i(z_i, \bar{P}_i, \bar{Q}_i). \tag{10}$$

In the above,  $\bar{I}_{inj,i} \in \mathbb{R}^2$  is the nominal injected current *i.e.* the control input of the nominal subsystem. Then, by defining the injected current of the true voltage dynamics (7) as a feedback control law of the form

$$I_{inj,i} = -K_i e_i + \bar{I}_{inj,i} \tag{11}$$

yields the dynamic model of the error subsystem

$$C_{i}\dot{e}_{d,i} = -K_{i}e_{d,i} + \omega_{g}C_{i}e_{q,i} - \mathcal{L}_{i}^{\top}e_{d}$$

$$-\frac{2}{3}\left(\frac{\bar{P}_{i}(e_{d,i}(e_{d,i} + z_{d,i}) + e_{q,i}^{2})}{z_{d,i}(e_{d,i} + z_{d,i})^{2} + z_{d,i}e_{q,i}^{2}}\right)$$

$$+\frac{\delta P_{i}(e_{d,i} + z_{d,i}) + \delta Q_{i}e_{q,i} - \bar{Q}_{i}e_{q,i}}{(e_{d,i} + z_{d,i})^{2} + e_{q,i}^{2}}\right), \quad (12a)$$

$$C_{i}\dot{e}_{q,i} = -K_{i}e_{q,i} - \omega_{g}C_{i}e_{d,i} - \mathcal{L}_{i}^{\top}e_{q}$$

$$-\frac{2}{3}\left(-\frac{\bar{Q}(e_{d,i}(e_{d,i} - z_{d,i}) - e_{q,i}^{2})}{z_{d,i}(e_{d,i} + z_{d,i})^{2} + z_{d,i}e_{q,i}^{2}}\right)$$

$$+\frac{-\delta Q_{i}(e_{d,i} + z_{d,i}) + \delta P_{i}e_{q,i} + \bar{P}_{i}e_{q,i}}{(e_{d,i} + z_{d,i})^{2} + e_{q,i}^{2}}\right). \quad (12b)$$

In order to simplify the adopted model, we have made the implicit assumption that the nominal voltage controller enforces  $z_{q,i}=0$  at all times. This is a common strategy in the literature of power systems, where we require one component of the d-q model to be identically zero, see [3]. The following sections will analytically present how this assumption can be enforced. However, it is important to highlight at this stage that, in the proposed control architecture, the nominal dynamics are uncertainty-free, *i.e.* it is substantially easier to satisfy the invoked assumption from a control perspective.

The original nodal capacitor dynamics have been restructured to a pair of d-q states described by (10) and (12) respectively. The aim of this paper is to design a unified control strategy, such that the nodal nominal solution operates as a reference trajectory for the true system, while the error is bounded in a compact set containing the origin.

## B. Control Objectives

The control objectives can be formulated as:

- 1) Guarantee the existence of a non-empty compact "safe" set  $S_i \subset \mathbb{R}^2$  containing the origin such that  $e_i(0) \in S_i$  implies  $e_i(t) \in S_i$ ,  $\forall t > 0$ .
- 2) Achieve  $\lim_{t\to\infty} z_i(t) = z_i^*$ , where  $z_i^* \in \mathbb{R}^2$  is a desired reference vector for the nodal nominal trajectory.
- 3) Ensure that if  $v_i(0) \in \mathbb{V}_i$  then  $v_i(t) \in \mathbb{V}_i$ ,  $\forall t > 0$ , where  $\mathbb{V}_i \subset \mathbb{R}^2$  is a set with strictly positive elements and is centred around a common rated voltage value  $v_i^o \in \mathbb{R}^2$ , where  $v_i^o = v_i^o$  for all  $(i,j) \in \mathcal{E}$ .

# IV. BOUNDEDNESS OF ERROR TRAJECTORY USING A CONTROL BARRIER FUNCTION

In this section, we aim to derive conditions on the magnitude of the feedback gain, such that the first control objective, defined in Section III-B, is satisfied. Essentially, this will enable a type of a "tube" behaviour of the true voltage dynamics, where the distance between the true and nominal voltage trajectories at each time instant determines the tube width. We are interested in the necessary conditions such that the tube width does not grow unbounded, which could possibly lead to unstable behaviour. Let  $\mathbb{D} \subset \mathbb{R}^2$  and consider a continuously differentiable quadratic function  $h \colon \mathbb{D} \to \mathbb{R}$  given by,

$$h_i(e_i) = e_i^{\top} e_i. \tag{13}$$

Furthermore, we define a continuously differentiable function  $b_i$ :  $\mathbb{D} \to \mathbb{R}$ , given by  $b_i(e_i) = \bar{e} - h(e_i)$ , where  $\bar{e} \in \mathbb{R}^2_{>0}$  has strictly positive elements. This allows us to define a

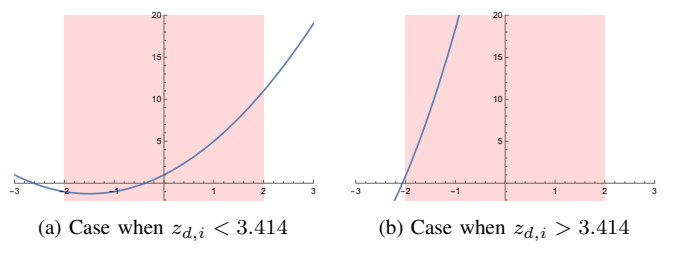


Fig. 1: Numerical illustration of Lemma 1, for  $\bar{e}=2$  with  $\bar{e}+\sqrt{\bar{e}}=3.414$ . Shaded region represents  $|e|\leq \bar{e}$ .

candidate positive invariant "safe" set as the  $\bar{e}$ -level set of  $h(\cdot)$  or equivalently,

$$S_i := \left\{ e_i \in \mathbb{R}^2 \colon \ b_i(e_i) \ge 0 \right\},\tag{14a}$$

$$\partial \mathcal{S}_i := \left\{ e_i \in \mathbb{R}^2 \colon \ b_i(e_i) = 0 \right\}.$$
 (14b)

Our aim is to show that the system vector field of any point on the boundary of the safe set is pointing inwards, and thus at any time instant  $\tau > 0$ , the intersection of the tube in d-q coordinates is given by  $S_i \oplus \{z_i(\tau)\}$ . This requirement can be formally stated by first defining the Lie derivative

$$\mathfrak{L}_{\dot{e}}b_i(e_i) := -\frac{\partial h_i(e_i)}{\partial e_i}\frac{de_i}{dt}.$$
 (15)

The task now becomes formulating sufficient conditions on the control law such that the above is non-negative, *i.e.*  $b(\cdot)$  is a CBF [34], [35]. Since we are only interested in showing positive invariance only of  $\mathcal{S}_i$ , as opposed to enforcing this condition on every sublevel set, we can relax the condition to investigate the definiteness of  $\inf_{e_i \in \partial \mathcal{S}_i} \left\{ \mathfrak{L}_{\dot{e}} b_i(e_i) \right\}$ . In other words, we investigate the behaviour of the network considering the states on the boundary of the set, in which case it holds that  $|e_i| \geq |e_j|$ ,  $\forall (i,j) \in \mathcal{E}$ . Exploiting this property yields the relation

$$\inf_{e_i \in \partial S_i} \left\{ \mathfrak{L}_{\dot{e}} b_i(e_i) \right\} \ge -\frac{\alpha_{nom,i}(e_i, z_i)}{\alpha_{den,i}(e_i, z_i)}. \tag{16}$$

where,

$$\begin{split} \alpha_{nom,i}(e_i,z_i) &= \\ e_{d,i}^4(-3K_iz_{d,i}) + e_{d,i}^3(-6K_iz_{d,i}^2 + 2\bar{P}_i) + \\ e_{d,i}^2e_{q,i}^2(-3K_iz_{d,i}) + e_{d,i}^2e_{q,i}(-3K_iz_{d,i} + 2\bar{Q}_i) + \\ e_{d,i}^2(-3K_iz_{d,i}^3 + 2\bar{P}_iz_{d,i} - 2\delta P_iz_{d,i}) + \\ e_{d,i}e_{q,i}^2(-6K_iz_{d,i}^2 + 2\bar{P}_i) + e_{d,i}e_{q,i}(-4\bar{Q}_iz_{d,i}) + \\ e_{q,i}^2(-3K_iz_{d,i}^3 - 2\bar{P}_iz_{d,i} - 2\delta P_iz_{d,i}) + \\ e_{q,i}^3(-3K_iz_{d,i} - 2\bar{Q}_i) + e_{d,i}(-2\delta P_iz_{d,i}^2) + \\ e_{q,i}(2\delta Q_iz_{d,i}^2). \end{split}$$

and

$$\alpha_{den,i} = z_{d,i} \left( (e_{d,i} + z_{d,i})^2 + e_{d,i} \right)$$
 (18)

The following collection of results will formulate sufficient conditions on the proposed control law (11), such that the right-hand-side of (16) is non-negative. The next Lemma investigates the definiteness of (18).

**Lemma 1.** For all  $i \in \mathcal{M}$ , if the nominal state satisfies

$$z_{d,i} > \bar{e} + \sqrt{\bar{e}},\tag{19}$$

then Image  $(\alpha_{den,i}) \subset \mathbb{R}_{>0}$ .

*Proof.* We will prove positive-definiteness of (18) directly from the properties of the function. First, we assume that  $z_{d,i} > 0$ , *i.e.* the d-component of the nominal voltage is strictly positive at all times. Setting the first derivative of the function to zero yields the extreme point,

$$\frac{\partial \alpha_{den,i}}{\partial e_{d,i}} = 0 \Rightarrow e_{d,i}^* = -\frac{z_{d,i}^2 + 0.5}{z_{d,i}}$$

which is strictly negative since  $z_{d,i} > 0$ . Furthermore, it is straightforward to show that the function is convex and thus  $e_{d,i}^*$  is a unique global minimizer. Assume, now, that (18) attains a negative value at the global minimum and thus obtains two real roots. In order to prove the Lemma statement, it is necessary to formulate a condition on the magnitude of the nominal voltage  $z_{d,i}$ , such that the largest real root of the function is smaller than the lower bound of the projection of  $S_i$  on d-axis. To formally state this, we require the largest root of  $\frac{\alpha_{den,i}}{z_{d,i}} = 0$  to satisfy

$$\frac{-2z_{d,i} + 1 + \sqrt{4z_{d,i} + 1}}{2} < -\bar{e},$$

which yields,

$$z_{d,i} > \bar{e} + \sqrt{\bar{e}}$$
.

**Corollary 1.** If (19) holds, then the nodal error dynamics in (12) are Lipschitz continuous over  $S_i$ .

The result of Lemma 1 is illustrated in Fig. 1. Setting the error bound at  $\bar{e}=2$  as an example, we can compute the lower bound on the nominal voltage by the statement of Lemma 1 as  $\bar{e}+\sqrt{\bar{e}}=3.414$ . It is seen that (18) obtains strictly positive values in the desired region when the lower bound is satisfied and changes sign only when  $z_{d,i}<3.414$ . The next result establishes a sufficient condition such that (17) is a negative definite function.

Lemma 2. If the feedback gain satisfies

$$K_i \ge \beta_i(e_i, z_i) \tag{20}$$

where  $\beta_i : \mathbb{R}^2 \times \mathbb{R}^2 \to \mathbb{R}$ ,

$$\beta_{i}(e_{i}, z_{i}) := \frac{1}{3} \frac{\frac{1+z_{d,i}}{z_{d,i}} \bar{P}_{i} + 2\bar{Q}_{i} + \frac{\bar{e}+z_{d,i}}{\bar{e}} \delta P_{\max,i} + \frac{z_{d,i}}{\bar{e}} \delta Q_{\max,i}}{(\bar{e}-z_{d,i})^{2} - \bar{e}}, \quad (21)$$

then for all  $e_i \in \partial S_i$  and  $i \in \mathcal{M}$  it holds that Image  $(\alpha_{nom,i}(e_i,z_i)) \subset \mathbb{R}_{<0}$ .

Proof. We begin this proof by rearranging (17) as,

$$\alpha_{nom,i}(e_i, z_i) = -3K_i f_K(e_i) + 2\bar{P}_i f_{\bar{P}}(e_i) + 2\bar{Q}_i f_{\bar{Q}}(e_i) - 2\delta P_i f_{\delta P}(e_i) + 2\delta Q_i f_{\delta O}(e_i)$$
 (22)

where,

$$f_K(e_i) = z_{d,i} e_{q,i} \left( e_{q,i}^2 + e_{q,i} \left( e_{d,i} + z_{d,i} \right)^2 + e_{d,i}^2 \right) + z_{d,i} e_{d,i}^2 \left( e_{d,i} + z_{d,i} \right)^2,$$
(23a)

$$f_{\bar{P}}(e_i) = e_{d,i}^3 + e_{d,i}^2 z_{d,i} + e_{d,i} e_{q,i}^2 - z_{d,i} e_{q,i}^2,$$
 (23b)

$$f_{\bar{Q}}(e_i) = e_{d,i}^2 e_{q,i} - 2z_{d,i} e_{d,i} e_{q,i} - e_{q,i}^3,$$
 (23c)

$$f_{\delta P}(e_i) = z_{d,i}e_{d,i}^2 + z_{d,i}e_{g,i}^2 + z_{d,i}^2e_{d,i},$$
 (23d)

$$f_{\delta Q}(e_i) = e_{q,i} z_{d,i}^2. \tag{23e}$$

Investigating the properties of  $f_K(\cdot)$ , it is straightforward to show that for  $e_i \in \partial S_i$  the function obtains strictly positive values. This follows from the fact that in the only case where  $f_K(\cdot)$  is not a sum of strictly positive functions is when  $e_{q,i} =$  $-\bar{e}_i$ . However, utilizing Lemma 1, the second summand of the first term remains strictly positive and dominates the other two terms inside the parenthesis. A second important property is that the function only vanishes at (0,0), which implies that  $f_K(\cdot)$  is continuously differentiable on  $\partial S_i$ . Thus, requiring (17) to be strictly negative can be guaranteed by the sufficient condition

$$K_{i} \geq \frac{2}{3 \min_{e_{i} \in \partial S_{i}} \{f_{K}(e_{i})\}} \left( \max_{e_{i} \in \partial S_{i}} \{\bar{P}_{i} f_{\bar{P}}(e_{i})\} + \max_{e_{i} \in \partial S_{i}} \{\bar{Q}_{i} f_{\bar{Q}}(e_{i})\} + \max_{e_{i} \in \partial S_{i}} \{\delta P_{max,i} f_{\delta P}(e_{i})\} + \max_{e_{i} \in \partial S_{i}} \{\delta Q_{\max,i} f_{\delta Q}(e_{i})\} \right)$$

It is noted that the above satisfy both conditions for the application of the Extreme Value Theorem; namely the set  $\partial S_i$  is compact and each individual function is continuous on this set. Therefore, there always exist at least one solution to each optimization problem. At the same time  $K_i$  is guaranteed to exist since  $f_K(\cdot)$  does not vanish on  $\partial S_i$ . Applying the lagrange method of multipliers to each individual optimization problem above computes the lower bound,

$$K_i \geq \frac{1}{3} \frac{\frac{1+z_{d,i}}{z_{d,i}} \bar{P}_i + 2\bar{Q}_i + \frac{\bar{e}+z_{d,i}}{\bar{e}} \delta P_{\max,i} + \frac{z_{d,i}}{\bar{e}} \delta Q_{\max,i}}{(\bar{e}-z_{d,i})^2 - \bar{e}}$$

Setting the right hand side to  $\beta_i(e_i, z_i)$  completes the proof.

Remark 1. Lemma 1 can be used to conclude that the lower bound on  $K_i$  is strictly positive. This follows from the fact that the nominator is a sum of strictly positive functions. Then, applying the condition of Lemma 1, it can be directly shown that the denominator attains strictly positive values.

We are now in position to establish positive invariance of (14) under the solution of the error dynamics. This property is proven in the next result.

**Proposition 1** (Boundedness of Error Dynamics). If the feedback gain of the control law in (11) satisfies (20) and at time t = 0 the initial condition of the error dynamics in (14)

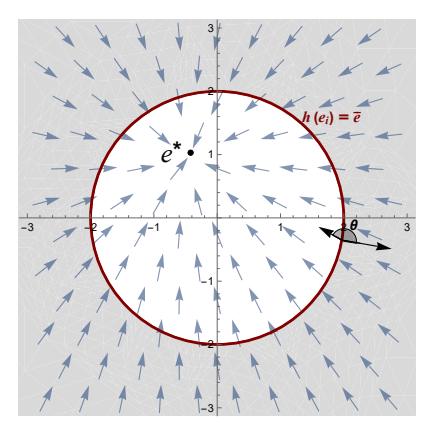


Fig. 2: Illustration of Proposition 1. For  $\theta$  denoting the angle between the normal vector on  $\partial \mathcal{S}$  and the system vector field at some point  $e_i \in \partial S$ , the derived conditions on  $z_{d,i}$  and  $K_i$  enforce  $|\theta| > \frac{\pi}{2}$ , i.e.  $S_i$  is a robust positive invariant. The tuning parameters used for this example are  $\bar{e} = 2V$  and K=6. The "unsafe" region is depicted by light grey.

satisfies  $e(0) \in S_i$  with set  $S_i$  defined in (14), then  $b \colon \mathbb{D} \to \mathbb{R}$ is a control barrier function with

$$\inf_{e_i \in \partial S_i} \left\{ \mathfrak{L}_{\dot{e}} b_i(e_i) \right\} \ge 0 \tag{24}$$

and the nodal error trajectories satisfy  $e_i(t) \in S_i$  for all  $t \ge 0$ 

*Proof.* By construction the set  $\partial S_i = h^{-1}(\{\bar{e}\})$  is closed, since it is defined as the pre-image of the closed set  $\{\bar{e}\}$ and  $h \colon \mathbb{R}^n \to \mathbb{R}$  is a continuously differentiable function. In addition, Lemma 1 guarantees Lipschitz continuity of the nodal error dynamics (12) over  $S_i$ . Considering Lemma 1 and Lemma 2 we deduce

$$\inf_{e_i \in \partial \mathcal{S}_i} \left\{ \mathfrak{L}_{\dot{e}} b_i(e_i) \right\} \ge -\frac{\alpha_{nom,i}(e_i, z_i)}{\alpha_{den,i}(e_i, z_i)} > 0, \ \forall i \in \mathcal{M}. \quad (25)$$

which implies that  $b(\cdot)$  is a control barrier function. Furthermore, the inner product between the error subsystem vectorfield and the respective normal vector satisfies

$$\langle \nabla h_i, \dot{e}_i \rangle |_{e_i \in \partial S_i} = -\mathfrak{L}_{\dot{e}} b_i(e_i)$$

$$\leq -\inf_{e_i \in \partial S_i} \left\{ \mathfrak{L}_{\dot{e}} b_i(e_i) \right\}$$
(26)

$$\leq -\inf_{e_i \in \partial S_i} \left\{ \mathfrak{L}_{\dot{e}} b_i(e_i) \right\} \tag{27}$$

$$\leq 0$$
 (28)

Therefore, all conditions of the Bony-Brezis Theorem are satisfied and the set  $\partial S_i$ , and by induction  $S_i$ , is positive invariant under the solution of the dynamics. This implies that any nodal trajectory starting at time t=0 satisfies  $e_i(0) \in \mathcal{S}_i$ , then  $e_i(t) \in \mathcal{S}_i, \forall t > 0$ . This concludes the proof.

The result of Proposition 1 is illustrated in Fig. 2. Satisfying the conditions on the nominal voltage and the feedback gain derived in Lemma 1 and Lemma 2 respectively, enforces positive invariance of the level-set  $S_i$  under the solution of the nodal error dynamics.

Following the guidelines formulated in this section guarantees that the first control objective is satisfied. The next sections are associated with the design of a constrained control architecture for the nominal dynamics that satisfy Lemma 1 and incorporate the desired operational constraints within the control designed process.

# V. CONSTRAINED REGULATION OF THE NOMINAL VOLTAGE DYNAMICS

In this section, a constrained control strategy is developed for the nominal dynamics. In order to satisfy the remaining control objectives, the proposed nominal controller is required to enforce a "tightened" bound on the nominal nodal trajectory such that the true state is enclosed within the desired bound at all times. Then, it is also desired to achieve fast regulation to a desired reference point and guarantee stability of the closed-loop dynamics in an analytic fashion. Considering Assumption 1 and the results of the previous section, it is necessary to satisfy

$$S_i \oplus Z_i \subseteq V_i,$$
 (29)

where  $\mathcal{Z}_i \subset \mathbb{R}^2$  is the constraint set for the nominal subsystem. To satisfy the above requirement, we first define a nominal rated voltage  $z_i^o = v_i^o$ . Then, shifting the nominal subsystem coordinates to a deviation from the rated value, i.e.  $\tilde{z} = z - z^o$  and  $\tilde{I}_{inj,i} = \bar{I}_{inj,i} - I_i^o$ , results in the shifted nominal subsystem

$$C_i \dot{\tilde{z}}_i = \tilde{I}_{inj,i} + J_2 \omega_g C_i \left( \tilde{z}_i + z_i^o \right) - \mathcal{L}_i^{\mathsf{T}} \tilde{z} - g_i \left( \tilde{z}_i + z_i^o, \bar{P}_i, \bar{Q}_i \right). \tag{30}$$

We note that  $I_i^o$  results from computing the equilibrium map of the nominal subsystem and substituting for the rated voltage. Therefore, the problem now becomes bounding the shifted nominal dynamics around the origin. To this aim, we propose the nominal control law defined as  $\tilde{I}_{inj,i}\colon \mathbb{R}^2 \times \mathbb{R}^2 \to \mathbb{R}^2$ , given by

$$\bar{I}_{inj,i} = \begin{bmatrix} -K_{d,i} & 0 \\ 0 & -K_{d,i} \end{bmatrix} \begin{bmatrix} \tilde{z}_{d,i} \\ \tilde{z}_{q,i} \end{bmatrix} + \begin{bmatrix} M_i & 0 \\ 0 & 1 \end{bmatrix} \begin{bmatrix} \sigma_{d,i} \\ \sigma_{q,i} \end{bmatrix} + \begin{bmatrix} \omega_{d,i} \\ \omega_{q,i} \end{bmatrix} + \begin{bmatrix} \omega_{d,i} \\ \omega_{q,i} \end{bmatrix} \begin{bmatrix} \omega_{d,$$

where  $\left[\sigma_{d,i} \ \sigma_{q,i}\right] \in \mathbb{R}^2$  are the respective d-q integrator states with dynamics given by

$$\dot{\sigma}_{d,i} = k_{Id,i} (1 - \sigma_{d,i}^2) (\hat{z}_{d,i} - \tilde{z}_{d,i}), \tag{32a}$$

$$\dot{\sigma}_{q,i} = -k_{Iq,i}\tilde{z}_{q,i}.\tag{32b}$$

In the above  $K_{d,i}, k_{Id,i}, M_i, K_{q,i}, k_{Iq,i} \in \mathbb{R}_{>0}$  are the controller tuning parameters for the respective d-q components, while  $\hat{z}_{d,i} \in \mathbb{R}$  denotes the desired shifted reference point. The remaining of this section is dedicated in providing the necessary theoretical analysis such that the adopted control law guarantees boundedness and stability of the nominal dynamics. The control law in (31) decouples the q-component of the nominal state from the d-component nominal dynamics. It is important to highlight that the adopted methodology allows such an assumption without requiring knowledge of the load demand, since in the nominal setting this is constant to a predefined value. Therefore, the load demand remains an unknown system disturbance in the original problem setting. The following result investigates the stability of the system

equilibria and derives necessary conditions on the tuning parameters to counteract the destabilizing effect of the CPL.

**Proposition 2** (Stability of Nominal Dynamics). *Consider the nodal nominal dynamics given by (10), (31) and (32) and an equilibrium point*  $\hat{x}_i = (\hat{z}_{d,i}, \hat{\sigma}_{d,i}, 0, 0)$ , if  $\hat{\sigma}_{d,i} \in (-1,1)$  and

$$K_{d,i} > \frac{2}{3} \frac{\bar{P}_i}{\hat{z}_{d\,i}^2},$$
 (33)

then the closed-loop nominal system (30) is asymptotically stable with respect to  $\hat{x}_i$ , for all  $i \in \mathcal{M}$ .

*Proof.* In order to derive asymptotic stability of the system equilibria, we study the network closed-loop nominal subsystem. With a slight abuse of notation these are given below,

$$[C]\dot{\tilde{z}}_d = -\left([K_d] + \mathcal{L}\right)\tilde{z}_d + [M]\sigma_d + [\omega_g C]\left(\tilde{z}_q + z_q^o\right) + g_d(\tilde{z} + z^o, \bar{P}, \bar{Q}), \quad (34a)$$

$$\dot{\sigma_d} = k_{Id} \left[ 1 - \sigma_d^2 \right] \left( \hat{z}_d - \tilde{z}_d \right), \tag{34b}$$

$$[C]\dot{z}_q = -(K_q + \mathcal{L})\,\tilde{z}_q + \sigma_q,\tag{34c}$$

$$\dot{\sigma}_q = k_{Iq} \tilde{z}_q. \tag{34d}$$

Considering an network equilibrium  $(\hat{z}_d, \hat{\sigma}_d, 0, 0)$ , the resulting Jacobian matrix of the system is given by (35). The resulting matrix is a block triangular matrix and it holds that  $\det(\lambda \mathbf{I_n} - J) = \det(\lambda \mathbf{I_n} - J_{11}) \det(\lambda \mathbf{I_n} - J_{22})$ , i.e., the eigenvalues are a combination of the block matrices on the diagonal [47], where

$$\mathcal{J}_{11} = \begin{bmatrix} [C]^{-1} \left( -[K_d] - \mathcal{L} + \left[ \frac{2}{3\hat{z}_d^2} \bar{P} \right] \right) & [C]^{-1}[M] \\ -[k_{Id}] \left[ 1 - \hat{\sigma}_d^2 \right] & \mathbf{0}_{n \times n} \end{bmatrix},$$
(36)

$$\mathcal{J}_{22} = \begin{bmatrix} -[K_q] - \mathcal{L} & \mathbf{I}_n \\ -[k_{Iq}] & \mathbf{0}_n \end{bmatrix}. \tag{37}$$

Therefore, if both  $\mathcal{J}_{11}$  and  $\mathcal{J}_{22}$  are Hurwitz then  $\mathcal{J}$  is also a Hurwitz matrix. Considering  $\mathcal{J}_{11}$ , the characteristic polynomial can be computed

$$\det\left(\lambda \mathbf{I_n} - \mathcal{J}_{11}\right) = \left|\lambda^2 \mathbf{I_n} + \lambda A + B\right| = 0 \tag{38}$$

where

$$A = [C]^{-1} \left( [K_d] + \mathcal{L} - \left[ \frac{2}{3\hat{z}_d^2} \bar{P} \right] \right)$$
 (39)

$$B = [C]^{-1}[M][k_{Id}] \left[1 - \hat{\sigma}_d^2\right]$$
 (40)

Right multiplying (38) by |[C]| yields

$$\left| [C] \lambda^2 \mathbf{I_n} + \lambda \mathbf{A} + \mathbf{B} \right| = 0, \tag{41}$$

where  $\mathbf{A} = [C]A$  and  $\mathbf{B} = [C]B$ . In the above, each coefficient is a symmetric matrix and thus the expression defines a Quadratic Eigenvalue Problem (QEP). According to the QEP theory [48], the eigenvalues are negative if each coefficient is positive definite. By construction,  $\mathbf{B}$  is a diagonal and positive definite matrix and it also holds that  $C \succ 0$ , thus we focus our attention on the second coefficient. By

$$\mathcal{J} = \begin{bmatrix}
[C]^{-1} \left( -[K_d] - \mathcal{L} + \left[ \frac{2}{3\tilde{z}_d^2} \bar{P} \right] \right) & [C]^{-1} M & \left[ \omega_g - \frac{2}{3\tilde{z}_d^2} \bar{Q} \right] & \mathbf{0}_n \\
-[k_{Id}] \left[ 1 - \hat{\sigma}_d^2 \right] & \mathbf{0}_n & \mathbf{0}_n & \mathbf{0}_n \\
\mathbf{0}_n & \mathbf{0}_n & -[K_q] - \mathcal{L} & \mathbf{I}_n \\
\mathbf{0}_n & \mathbf{0}_n & \left[ k_{Iq} \right] & \mathbf{0}_n
\end{bmatrix} \tag{35}$$

the properties of a Laplacian matrix [49], it holds that the respective eigenvalues satisfy  $\lambda_1 = 0 < \lambda_2 \le \cdots \le \lambda_n$ , and thus  $\lambda_{\min}(-\mathcal{L}) = 0$ . Considering that the rest of the summands of **A** are diagonal matrices, the smallest eigenvalue  $\lambda_{\max}(\mathbf{A})$ , corresponding to some ith node, is given by

$$\lambda_{\max}(\mathbf{A}) = K_{d,i} - \frac{2}{3} \frac{\bar{P}_i}{\hat{z}_{d,i}^2}.$$
 (42)

Therefore, the condition  $\lambda_{\max}(\mathbf{A}) < 0$  yields

$$K_{d,i} > \frac{2}{3} \frac{\bar{P}_i}{\hat{z}_{d,i}^2}.$$
 (43)

Satisfying the above implies that  $\mathcal{J}_{11}$  is a Hurwitz matrix. A similar methodology can be used to prove  $\mathcal{J}_{22}$  is also Hurwitz under the condition that  $K_{q,i} > 0$  holds for all  $i \in \mathcal{M}$ . Therefore  $\mathcal{J}$  is also Hurwitz, since its eigenvalues are given as a combination of  $\mathcal{J}_{11}$  and  $\mathcal{J}_{22}$ . Therefore, the closed-loop system admits asymptotically stable equilibria in  $\mathbb{V}$ . This concludes the proof.

The closed-loop nominal subsystem admits asymptotically stable equilibria as long as condition (33) holds. Nevertheless, on of the control objectives is to guarantee that the local bus voltage adheres to desired operational constraints. Proposition 2 guarantees that there exist a local Lyapunov function and thus every subset of the respective domain is positive invariant; However, this result holds only locally in a neighbourhood of the respective equilibrium point. Therefore, the above are not sufficient to guarantee positive invariance of  $\mathcal{Z}_i$  under the solution of the nominal nodal dynamics. The desired property is proven in the following result.

**Proposition 3** (Boundedness of Nominal Voltage). *Consider a nominal voltage constraint set defined as* 

$$\mathcal{Z} := \prod_{i \in \mathcal{M}} \mathcal{Z}_i, \tag{44}$$

with

$$\mathcal{Z}_i := \left\{ \tilde{z}_i \in \mathbb{R}^2 \colon \ \tilde{z}_{q,i} = 0, \ -\delta_i - \tilde{z}_{\mathsf{m}} \le \tilde{z}_{d,i} \le \tilde{z}_{\mathsf{m},i} \right\}, \tag{45}$$

for some  $\delta_i > 0$  and  $\tilde{z}_{m,i} = \frac{M_i}{K_{d,i}}$ . If at time t = 0 the initial conditions satisfy  $z_i(0) \in \mathcal{Z}_i$  and  $\sigma_{d,i}(0) \in (-1,1)$ , and

$$K_{d,i} \ge \frac{2}{3} \frac{\bar{P}_i}{\delta_i \left( z_i^o - \tilde{z}_{\text{m},i} - \delta_i \right)},\tag{46}$$

holds for all  $i \in \mathcal{M}$ , then for all future times t > 0, the nominal system states satisfy  $\tilde{z}_i(t) \in \mathcal{Z}_i$  and  $\sigma_{d,i}(t) \in (-1,1)$ 

*Proof.* The proof of this result will be provided in two steps, showing first boundedness of the d-component integrator

dynamics and using this property to prove boundedness of the nominal voltages. The first part will be proven by contradiction. Consider the continuously differentiable integrator dynamics from (32a). Let there exist a time instant  $\tau_2$  such that the respective solution satisfies  $|\sigma_{d,i}(\tau_2)| > 1$ . Continuity of the dynamics imply that there exists a time instant  $\tau_1$  such that  $|\sigma_{d,i}(\tau_1)| = 1$ , and, furthermore,  $\theta_1, \theta_2 > 0$  such that  $|\sigma_{d,i}(\tau_1 - \theta_1)| < 1$  and  $|\sigma_{d,i}(\tau_1 + \theta_2)| > 1$ , i.e. the solution enters and leaves the set boundary defined at  $|\sigma_{d,i}(t)| = 1$ . Nevertheless, the point  $|\sigma_{d,i}(t)| = 1$  is an equilibrium point of the integrator dynamics, attracting or repelling the respective trajectories. This leads to a contradiction and thus for every possible trajectory with initial condition  $\sigma_{d,i}(0) \in (-1,1)$  it holds that  $\sigma_{d,i}(t) \leq (-1,1)$ ,  $\forall t \geq 0$ .

In order to prove boundedness of the nominal voltage, we first note that Proposition 2 implies that  $z_{q,i}(t) = 0$ , for all t > 0, since  $z_{q,i}(0) = 0$ . This creates a one dimensional constraint set on the d-component of the nominal voltage, that, by construction, is closed and bounded. Similarly to the previous section, we will show set invariance using the inner product of the system vector field and the outside normal vector on the boundary of the constraint set. In regards to the upper bound this yields,

$$\left\langle \dot{\bar{z}}_{d,i}, 1 \right\rangle \Big|_{\bar{z}_{d,i} = \bar{z}_{m,i}} = -M_i + M_i \sigma_i - \frac{\bar{P}_i}{\bar{z}_{m,i} + z_i^o} - \mathcal{L}_i^{\top} \frac{M_i}{K_{d,i}}$$

$$\leq 0$$

Similarly, the inner product at the lower boundary is computed as

$$\left\langle \dot{\tilde{z}}_{d,i}, -1 \right\rangle \Big|_{\tilde{z}_{d,i} = -\tilde{z}_{m,i} - \delta_i} = -K_{d,i}\delta_i + \frac{2}{3} \frac{\bar{P}_i}{-\tilde{z}_{m,i} - \delta_i + z_i^o}.$$

In order for the inner product to be negative, we deduce the condition

$$K_{d,i} \ge \frac{2}{3} \frac{\bar{P}_i}{\delta_i \left( z_i^o - \tilde{z}_{m,i} - \delta_i \right)}.$$
 (47)

Therefore, both conditions of the Bony-Brezis Theorem are satisfied; *i.e.* the system solutions are unique and continuous and the inner product on the boundary of the desired set is non-positive. Therefore, we can conclude that  $\mathcal{Z}_i$  is positive invariant under the solution of the nominal nodal dynamics and by direct extension  $\mathcal{Z}$  is positive invariant with respect to the network nominal dynamics.

Remark 2. Considering the theoretic results of this section, the feedback gain  $K_{d,i}$  needs to be chosen to satisfy both conditions of Propositions 2 and 3, *i.e.* 

$$K_{d,i} \ge \frac{2}{3} \max \left\{ \frac{\bar{P}_i}{\left(-\tilde{z}_{\mathsf{m},i} - \delta_i\right)^2}, \ \frac{\bar{P}_i}{\delta_i \left(z_i^o - \tilde{z}_{\mathsf{m},i} - \delta_i\right)} \right\}$$
(48)

Remark 3. The purpose of the parameter  $\delta_i$  is to quantify the necessary feedback gain that counteracts voltage drop caused by the CPL. Specifically, Proposition 3 indicates that smaller values of  $\delta_i$  require larger values of the feedback gain to achieve boundedness of the dynamics. The reasoning behind this, and the necessity of  $\delta_i$ , lies within the details of the proof of Prop. 3, where in order to derive the condition (47) we require a non-positive inner product on the boundary of the set. If the set was not parametrized by  $\delta_i$ , then it is not possible to establish a finite bound on  $K_{d,i}$ , or simply we would require an infinite gain for  $\delta_i = 0$ .

## VI. STABILITY OF THE CASCADED SYSTEM

By collecting the results of the previous sections, the original system dynamics in (7) are now represented by the equivalent system model described by (12) and (30). The new cascaded structure describes the true voltage trajectory v(t) as a summation of the respective error and nominal trajectories, *i.e.* v(t) = e(t) + z(t). The former was transformed in a shifted form to allow us to bound the nominal subsystem within a positive invariant set with strictly positive elements. Ultimately, the network voltage trajectories are given by

$$v(t) = e(t) + \tilde{z}(t) + z^{o}, \tag{49}$$

The only remaining requirement is combining the theoretic results of the previous sections to guarantee asymptotic stability of the cascaded dynamics with solutions described by the right-hand side of (49). Due to the presence of the nonconstant load demand, it is required to describe the stability properties with respect to an equilibrium *set* rather than an equilibrium *point*. To this end, we define an equilibrium set for the cascaded network dynamics  $\Omega \subseteq \mathbb{R}^{6n}$  given by

$$\Omega := \left\{ \left( e, \tilde{z}, \sigma_d, \sigma_q \right) \in \mathbb{R}^{6n} : e \in \mathcal{S}, \ \tilde{z} = \left( \hat{z}_d, 0 \right)^\top, \sigma_d = \hat{\sigma}_d, \ \sigma_q = 0 \right\}, \quad (50)$$

where

$$\hat{\sigma}_d = [M]^{-1} ([K_d] + \mathcal{L})^{-1} \hat{z}_d - g_d (\hat{z} + z^o, \bar{P}, \bar{Q}).$$
 (51)

The asymptotic stability of the network dynamics with respect to  $\Omega$  is proven in the next result.

**Theorem 2** (Stability of Network Dynamics). The network dynamics described by (12) and (30) are asymptotically stable with respect to the equilibrium set  $\Omega$  and  $\lim_{t\to\infty} v(t) = z^o + (\hat{z}, 0)^\top + e(t)$ , with  $e(t) \in \mathcal{S}$ .

*Proof.* Leveraging the results of Prop. 2, the nominal dynamics (30) admit a single asymptotically stable equilibrium in  $\mathcal{Z}$  and  $\mathcal{Z}$  is positive invariant under the solution of the dynamics. Therefore, the nominal voltage trajectory converges to the respective equilibrium for any  $z(0) \in \mathcal{Z}$ . Furthermore, Prop. 1 guarantees that  $b(\cdot)$  is a CBF and  $\mathcal{S}$  is a robust positive invariant set, such that for all  $e(0) \in \mathcal{S}$  and any  $\delta P \in \mathbb{W}_P$ ,  $\delta Q \in \mathbb{W}_Q$ , the respective solution remains within the set  $\mathcal{S}$  for all future times. Therefore, the above allows us to adopt a driving-driven cascaded system approach, see [50], where the cascaded dynamics are an interconnection between a

driving asymptotically stable subsystem and a driven bounded subsystem. Hence, we conclude that the true voltage network system is asymptotically stable with respect to the equilibrium set  $\Omega$  and the respective trajectory converges to  $\Omega$  in finite time.

Furthermore, the following Corollary can be deduced by leveraging the fact that there exist a single unique equilibrium set within the interior of  $\mathbb{V}$ .

**Corollary 2.** An estimate for the region of attraction of the closed-loop cascaded dynamics equilibrium set is given by  $int(\mathbb{V})$ .

The algorithm describing the methodology of tuning the proposed controller is outlined bellow.

## Algorithm Control Design Procedure

- 1: Specify desired quadratic error bound  $\bar{e}_i \in \mathbb{R}^2_{>0}$  and design error feedback gain according to (20).
- 2: Specify  $\tilde{z}_{\mathrm{m}}$  and  $\delta_{i}$  such that  $\mathcal{Z}_{i} \oplus \mathcal{S}_{i} \subseteq \mathbb{V}_{i}$  and (19) hold for all  $i \in \mathcal{M}$ .
- 3: Design  $K_{d,i}$  according to (48) and  $M_i$  to satisfy  $M_i = \tilde{z}_{\rm m} K_{d,i}$ .

## VII. ILLUSTRATIVE EXAMPLE

This section will demonstrate the operation of the closed-loop system, illustrating the theoretic properties established in the previous sections. An AC Microgrid network is considered with topology depicted in Fig. 3. The Microgrid consists of six local buses, each connected to a local DG unit and a CPL. Each CPL is assumed to acquire nominal active and reactive load values at  $\bar{P}_i = 500$  W and  $\bar{Q}_i = 400$  Var, with maximum load demand perturbations  $|\delta P_i| = 500$  W and  $|\delta Q_i| = 400$  Var respectively. In order to demonstrate the boundedness property of the closed-loop system trajectories, the desired voltage constraint set for each node is chosen for the RMS voltage as  $\mathbb{V}_i = \{v_{\mathrm{rms},i} \in \mathbb{R} \colon 103.5 \leq v_{\mathrm{rms},i} \leq 115.5\}$ . We choose  $\bar{e} = 0.2$  which results in  $\|v_i\| \leq \|z_i\| + \sqrt{\bar{e}}$ , i.e. the maximum distance between the nodal RMS voltage and the reference trajectory is  $\max \left\{ \mathrm{dist} \left( \|v_i\|, \|z_i\| \right) \right\} = \sqrt{\bar{e}}$ .

## A. Two Nodes Interaction

Initially, we focus our attention on the interaction between two neighbouring nodes, considering a scenario where the nominal voltage subsystem is regulated from  $z_{\rm rms,1}=z_{\rm rms,2}=110\,{\rm V}$  via subsequent reference changes to values on the boundary of the respective nominal constraint set  $\mathcal{Z}_i=\{z_{\rm rms,i}\in\mathbb{R}\colon\ 104\le z_{\rm rms,i}\le 115\}$ . The system trajectory is depicted in Fig. 4, showing constraint satisfaction at all times for both the true and the nominal voltage subsystems. The tube-control property of the cascaded system is also illustrated via the tube cross-sections at different time intervals. It is shown that the true nodal voltage trajectory is always bounded within the respective tube.

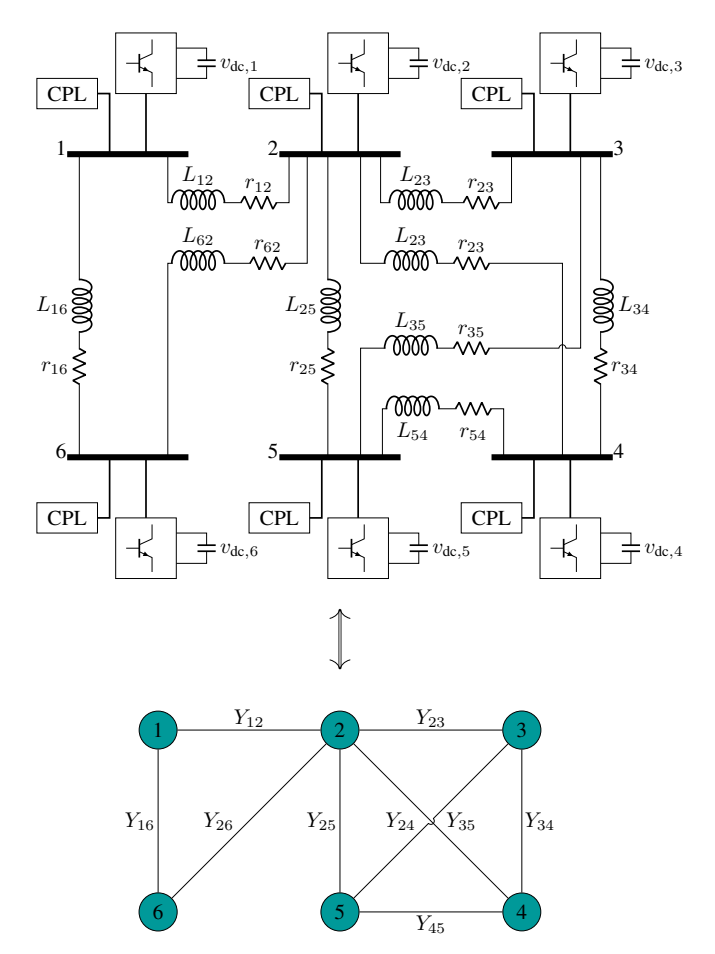


Fig. 3: *Top*: Single-phase equivalent of the adopted meshed Microgrid network with six local buses *Bottom*: Equivalent weighted graph with six nodes and nine edges.

## B. Microgrid Network

A similar scenario is investigated, this time considering the entire network system. It is assumed that a voltage reference vector is provided by a supervisory layer to achieve a desired economical operation. At time  $t = 0 \,\mathrm{s}$  the network system is operating within an equilibrium set, with nominal RMS reference vector  $\hat{z}_i = \{106.5 \ 108 \ 109.5 \ 111.5 \ 113 \ 114.5\} \text{ V},$ see Fig. 5. Similarly to the previous case, the controller enforces boundedness on the distance between the true and the nominal subsystem trajectories in the respective control tubes. Then, at time  $t = 0.2 \,\mathrm{s}$  a reference change occurs with  $\hat{z}_i = \{105\ 106.5\ 108\ 109.5\ 111\ 112.5\}\,\mathrm{V}$ , and the network converges to the new equilibrium set. A second reference change happens at  $t = 0.4 \,\mathrm{s}$ , where, this time, the provided setpoint of the 6th node lies outside the constraint set, namely  $\hat{z}_i = \{109\ 110.5\ 112\ 113.5\ 115\ 116\}\,\mathrm{V}$ . The respective integrator trajectories of the d-component nominal voltage are shown in Fig. 6. In the cases where the setpoints are on or outside the boundary of the nominal voltage constraint set, the integrator trajectories converge to the boundary of [-1, 1], and, a property that was proven in Proposition 3. This enforces the desired constraint on the RMS value of the nominal voltage trajectories.

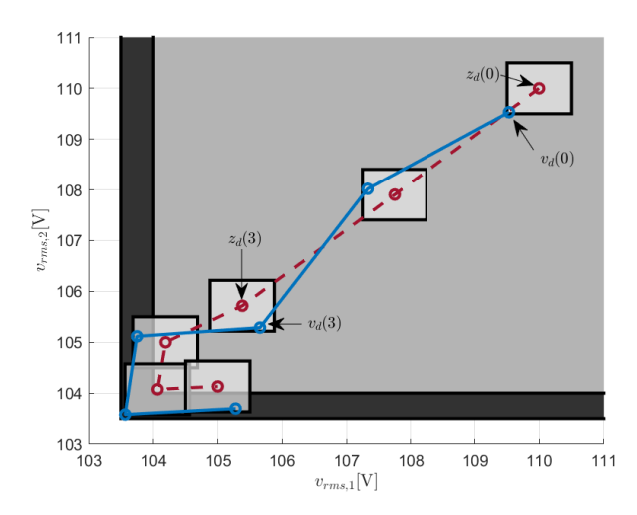


Fig. 4: True and nominal voltage trajectories for Node 1 and Node 2. Cross-sections of the tube are depicted in different time instants. The nominal constraint set  $\mathcal{Z}_1 \times \mathcal{Z}_2$  is depicted by light gray, while the true voltage constraint set  $\mathbb{V}_1 \times \mathbb{V}_2$  by dark grey.

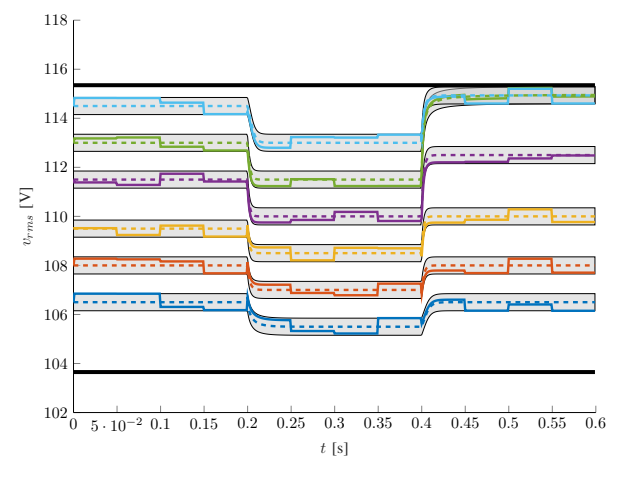


Fig. 5: Network true and nominal voltage trajectories for Node 1 (—,---), Node 2 (—,---), Node 3 (—,---), Node 4 (—,---), Node 5 (—,---), and Node 6 (—,---) respectively. The lower and upper bound of the constraint set are depicted with black solid lines. The control tube for each node is depicted by light gray.

Considering the load perturbations of Node 1 in in Fig. 7 and Fig. 8 respectively, the evolution of the control barrier function over the trajectory is depicted in Fig. 9. It can be observed that the function is strictly positive despite the presence of maximum disturbance values. Ultimately, the proposed controller successfully bounds the true voltage within the desired constraint region, demonstrating system robustness to both inconsistent setpoints and load demand perturbations.

## VIII. CONCLUSIONS

This study investigates the voltage regulation problem of an AC Microgrid network with high penetration of CPLs in the network. The mathematical analysis follows a reformulation

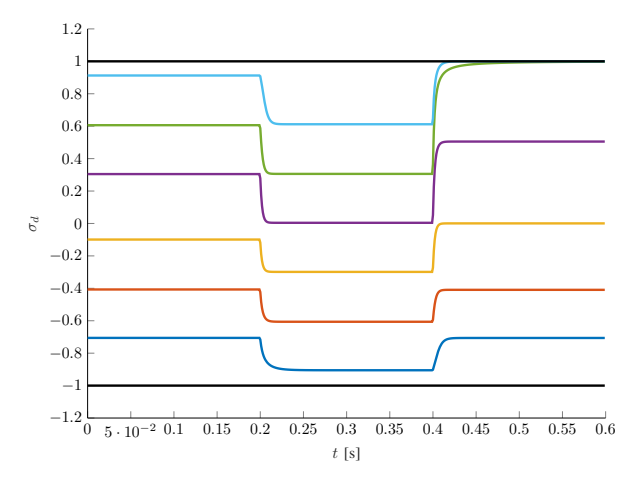


Fig. 6: Integrator state trajectories of the d-component nominal voltage of Node 1 (—), Node 2 (—,), Node 3 (—), Node 4 (—), Node 5 (—), and Node 6 (—) respectively. The lower and upper bounds of the integrator constraint are depicted by black solid lines.

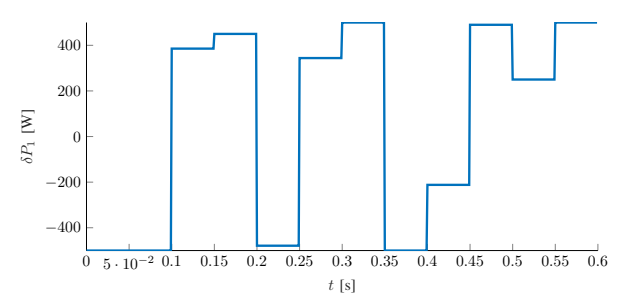


Fig. 7: Active power demand fluctuation of Node 1.

of the d-q network dynamics to a cascaded system composed by a nominal and an error subsystem. In the former, a known constant load demand is assumed, while the latter captures the error between the true and the nominal voltage trajectories. Necessary and sufficient conditions are analytically formulated to guarantee the existence of a robust positive invariant set  $\mathcal S$  under the solution of the error dynamics through the adoption of suitable control barrier functions. Then, a nonlinear PI controller was proposed to achieve constrained regulation of the nominal voltage dynamics to desired references. It was proven that the true voltage trajectories satisfy  $v(t) \in \{z(t)\} \oplus \mathcal S$  at all times. Furthermore, constrained regulation of the true voltage RMS value with respect to a set  $\mathbb V$  was demonstrated in an simulation scenario.

The mathematical analysis of this paper provided an insight on the interaction between the nonlinear load and the proposed controller parameters. This methodology allowed, firstly, a characterization of the CPL effect on the closed-loop system vector field. Subsequently, this knowledge was exploited to derive appropriate conditions on the magnitude of the controller tuning parameters such that the cascaded system admits asymptotically stable equilibria and satisfies the desired operational constraints. Future works will aim to address the conservativeness on the size of the safe set, rising from always assuming a worst-case scenario on the value

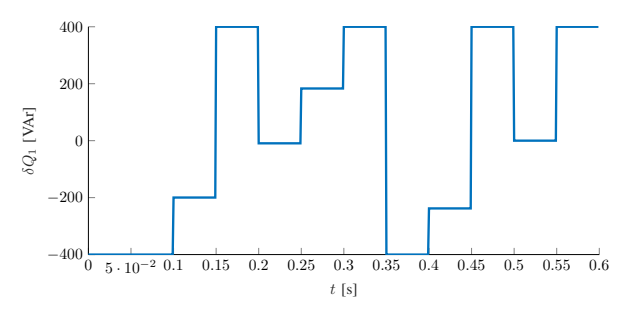


Fig. 8: Reactive power demand fluctuation of Node 1.

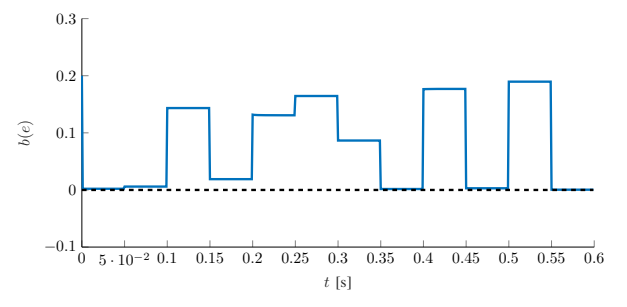


Fig. 9:  $b(e_1)$  over the error trajectory of Node 1.

of the nominal trajectory. Furthermore, it is also necessary to investigate the adoption of a supervisory controller that exploits the properties of the primary control system and achieves economic operation.

# REFERENCES

- [1] F. Dörfler and D. Groß, "Control of low-inertia power systems," *Annual Review of Control, Robotics, and Autonomous Systems*, vol. 6, no. 1, pp. 415–445, 2023.
- [2] M. C. Chandorkar, D. M. Divan, and R. Adapa, "Control of parallel connected inverters in standalone ac supply systems," *IEEE transactions* on industry applications, vol. 29, no. 1, pp. 136–143, 2002.
- [3] S. D'Arco, J. A. Suul, and O. B. Fosso, "A virtual synchronous machine implementation for distributed control of power converters in smartgrids," *Electric Power Systems Research*, vol. 122, pp. 180–197, 2015.
- [4] D. Groß, M. Colombino, J.-S. Brouillon, and F. Dörfler, "The effect of transmission-line dynamics on grid-forming dispatchable virtual oscillator control," *IEEE Transactions on Control of Network Systems*, vol. 6, no. 3, pp. 1148–1160, 2019.
- [5] N. Pogaku, M. Prodanovic, and T. C. Green, "Modeling, analysis and testing of autonomous operation of an inverter-based microgrid," *IEEE Transactions on power electronics*, vol. 22, no. 2, pp. 613–625, 2007.
- [6] C. Alfaro, R. Guzman, L. G. De Vicuna, H. Komurcugil, and H. Martin, "Distributed direct power sliding-mode control for islanded ac microgrids," *IEEE transactions on industrial electronics*, vol. 69, no. 10, pp. 9700–9710, 2021.
- [7] P. Vorobev, P.-H. Huang, M. Al Hosani, J. L. Kirtley, and K. Turitsyn, "High-fidelity model order reduction for microgrids stability assessment," *IEEE Transactions on Power Systems*, vol. 33, no. 1, pp. 874–887, 2017.
- [8] R. H. Lasseter, Z. Chen, and D. Pattabiraman, "Grid-forming inverters: A critical asset for the power grid," *IEEE Journal of Emerging and Selected Topics in Power Electronics*, vol. 8, no. 2, pp. 925–935, 2019.
- [9] A. Khan, M. M. Khan, Y. Li, J. Chuanwen, M. U. Shahid, and I. Khan, "A robust control scheme for voltage and reactive power regulation in islanded ac microgrids," *Electric Power Systems Research*, vol. 210, p. 108179, 2022.
- [10] M. Rasheduzzaman, J. A. Mueller, and J. W. Kimball, "Reducedorder small-signal model of microgrid systems," *IEEE Transactions on Sustainable Energy*, vol. 6, no. 4, pp. 1292–1305, 2015.

- [11] S. M. Mohiuddin and J. Qi, "Droop-free distributed control for ac microgrids with precisely regulated voltage variance and admissible voltage profile guarantees," *IEEE Transactions on Smart Grid*, vol. 11, no. 3, pp. 1956–1967, 2019.
- [12] U. Markovic, O. Stanojev, P. Aristidou, E. Vrettos, D. Callaway, and G. Hug, "Understanding small-signal stability of low-inertia systems," *IEEE Transactions on Power Systems*, vol. 36, no. 5, pp. 3997–4017, 2021.
- [13] R. Ofir, U. Markovic, P. Aristidou, and G. Hug, "Droop vs. virtual inertia: Comparison from the perspective of converter operation mode," in 2018 IEEE International Energy Conference (ENERGYCON). IEEE, 2018, pp. 1–6.
- [14] J. Schiffer, R. Ortega, A. Astolfi, J. Raisch, and T. Sezi, "Conditions for stability of droop-controlled inverter-based microgrids," *Automatica*, vol. 50, no. 10, pp. 2457–2469, 2014.
- [15] J. Schiffer, D. Efimov, and R. Ortega, "Global synchronization analysis of droop-controlled microgrids—a multivariable cell structure approach," *Automatica*, vol. 109, p. 108550, 2019.
- [16] X. He, V. Häberle, I. Subotić, and F. Dörfler, "Nonlinear stability of complex droop control in converter-based power systems," *IEEE Control* Systems Letters, vol. 7, pp. 1327–1332, 2023.
- [17] I. Subotić, D. Groß, M. Colombino, and F. Dörfler, "A lyapunov framework for nested dynamical systems on multiple time scales with application to converter-based power systems," *IEEE Transactions on Automatic Control*, vol. 66, no. 12, pp. 5909–5924, 2020.
- [18] J. Choi, S. I. Habibi, and A. Bidram, "Distributed finite-time event-triggered frequency and voltage control of ac microgrids," *IEEE Transactions on Power Systems*, vol. 37, no. 3, pp. 1979–1994, 2021.
- [19] S. Arora, P. Balsara, and D. Bhatia, "Input-output linearization of a boost converter with mixed load (constant voltage load and constant power load)," *IEEE Transactions on Power Electronics*, vol. 34, no. 1, pp. 815–825, 2018.
- [20] G. Michos, P. R. Baldivieso-Monasterios, G. C. Konstantopoulos, and P. A. Trodden, "Robust two-layer control of dc microgrids with fluctuating constant power load demand," *IEEE Transactions on Control of Network Systems*, vol. 11, no. 1, pp. 427–438, 2023.
- [21] G. Michos, G. C. Konstantopoulos, and P. A. Trodden, "Dynamic tube control for dc microgrids," *IEEE Control Systems Letters*, 2024.
- [22] A.-C. Braitor, H. Siguerdidjane, and A. Iovine, "On the voltage stability and network scalability of onboard dc microgrids for hybrid electric aircraft," *IEEE Transactions on Aerospace and Electronic Systems*, 2024.
- [23] K. Areerak, T. Sopapirm, S. Bozhko, C. I. Hill, A. Suyapan, and K. Areerak, "Adaptive stabilization of uncontrolled rectifier based acdc power systems feeding constant power loads," *IEEE Transactions on Power Electronics*, vol. 33, no. 10, pp. 8927–8935, 2017.
- [24] M. Mahdavyfakhr, N. Amiri, H. Lin, and J. Jatskevich, "Dynamic analysis of ac microgrids with constant power loads or sources," in 2021 IEEE Energy Conversion Congress and Exposition (ECCE). IEEE, 2021, pp. 238–244.
- [25] M. Molinas, D. Moltoni, G. Fascendini, J. A. Suul, and T. Undeland, "Constant power loads in ac distribution systems: An investigation of stability," in 2008 IEEE international symposium on industrial electronics. IEEE, 2008, pp. 1531–1536.
- [26] Z. Liu, J. Liu, W. Bao, Y. Zhao, and F. Liu, "A novel stability criterion of ac power system with constant power load," in 2012 Twenty-Seventh Annual IEEE Applied Power Electronics Conference and Exposition (APEC). IEEE, 2012, pp. 1946–1950.
- [27] M. Molinas, D. Moltoni, G. Fascendini, J. Suul, R. Faranda, and T. Undeland, "Investigation on the role of power electronic controlled constant power loads for voltage support in distributed ac systems," in 2008 IEEE Power Electronics Specialists Conference. IEEE, 2008, pp. 3597–3602.
- [28] Z. Liu, J. Liu, W. Bao, and Y. Zhao, "Infinity-norm of impedance-based stability criterion for three-phase ac distributed power systems with constant power loads," *IEEE Transactions on Power Electronics*, vol. 30, no. 6, pp. 3030–3043, 2014.
- [29] P. Mansoorhoseini, B. Mozafari, and S. Mohammadi, "Islanded ac/dc microgrids supervisory control: A novel stochastic optimization approach," *Electric Power Systems Research*, vol. 209, p. 108028, 2022.
- [30] J. Zhou, H. Sun, Y. Xu, R. Han, Z. Yi, L. Wang, and J. M. Guerrero, "Distributed power sharing control for islanded single-/three-phase microgrids with admissible voltage and energy storage constraints," *IEEE Transactions on Smart Grid*, vol. 12, no. 4, pp. 2760–2775, 2021.
- [31] L. Kölsch, K. Wieninger, S. Krebs, and S. Hohmann, "Distributed frequency and voltage control for ac microgrids based on primal-dual gradient dynamics *IFAC-PapersOnLine*, vol. 53, no. 2, pp.

- 12 229–12 236, 2020, 21st IFAC World Congress. [Online]. Available: https://www.sciencedirect.com/science/article/pii/S2405896320314877
- [32] M. Mottaghizadeh, F. Aminifar, T. Amraee, and M. Sanaye-Pasand, "Robust fuzzy model predictive control for voltage regulation in islanded microgrids," *IET Generation, Transmission & Distribution*, vol. 16, no. 5, pp. 1013–1029, 2022.
- [33] T. E. Kavvathas and G. C. Konstantopoulos, "Novel virtual synchronous generator design with dynamic virtual inertia and bounded frequency, current and voltage characteristics," *IEEE Transactions on Sustainable Energy*, pp. 1–14, 2025.
- [34] A. D. Ames, X. Xu, J. W. Grizzle, and P. Tabuada, "Control barrier function based quadratic programs for safety critical systems," *IEEE Transactions on Automatic Control*, vol. 62, no. 8, pp. 3861–3876, 2016.
- [35] X. Xu, P. Tabuada, J. W. Grizzle, and A. D. Ames, "Robustness of control barrier functions for safety critical control," *IFAC-PapersOnLine*, vol. 48, no. 27, pp. 54–61, 2015.
- [36] Z. Wu and H. Cheng, "Fixed-time control of distributed secondary voltage and frequency for microgrids considering state-constrained," *Electrical Engineering*, vol. 106, no. 3, pp. 2637–2649, 2024.
- [37] K. Hassan, D. Selvaratnam, and H. Sandberg, "On resilience guarantees by finite-time robust control barrier functions with application to power inverter networks," *IEEE Open Journal of Control Systems*, 2024.
- [38] S. Kundu, S. Geng, S. P. Nandanoori, I. A. Hiskens, and K. Kalsi, "Distributed barrier certificates for safe operation of inverter-based microgrids," in 2019 American Control Conference (ACC). IEEE, 2019, pp. 1042–1047.
- [39] S. I. Habibi and A. Bidram, "Unfalsified switching adaptive voltage control for islanded microgrids," *IEEE Transactions on Power Systems*, vol. 37, no. 5, pp. 3394–3407, 2021.
- [40] S. Ullah, L. Khan, I. Sami, and J. Ro, "Voltage/frequency regulation with optimal load dispatch in microgrids using smc based distributed cooperative control," *IEEE Access*, vol. 10, pp. 64873–64889, 2022.
- [41] G. Michos, G. C. Konstantopoulos, P. A. Trodden, and V. Kadirka-manathan, "Control of isolated ac microgrids with constant power loads: A set invariance approach," in 2023 31st Mediterranean Conference on Control and Automation (MED). IEEE, 2023, pp. 239–244.
- [42] R. Redheffer, "The theorems of bony and brezis on flow-invariant sets," The American Mathematical Monthly, vol. 79, no. 7, pp. 740–747, 1972.
- [43] J. Espinoza, G. Joos, and P. Ziogas, "Voltage controlled current source inverters," in *Proceedings of the 1992 International Conference on In*dustrial Electronics, Control, Instrumentation, and Automation. IEEE, 1992, pp. 512–517.
- [44] Y. Ojo, J. D. Watson, K. Laib, and I. Lestas, "A distributed scheme for voltage and frequency control and power sharing in inverter-based microgrids," *IEEE Transactions on Control Systems Technology*, vol. 31, no. 4, pp. 1679–1691, 2023.
- [45] P. R. Baldivieso-Monasterios and G. C. Konstantopoulos, "Constrained control for microgrids with constant power loads," in 2020 59th IEEE Conference on Decision and Control (CDC). IEEE, 2020, pp. 3341– 3346
- [46] H. K. Khalil and J. W. Grizzle, *Nonlinear systems*. Prentice hall Upper Saddle River, NJ, 2002, vol. 3.
- [47] S. Axler, Linear algebra done right. Springer Nature, 2024.
- [48] F. Tisseur and K. Meerbergen, "The quadratic eigenvalue problem," SIAM review, vol. 43, no. 2, pp. 235–286, 2001.
- [49] F. Bullo, J. Cortés, F. Dörfler, and S. Martínez, Lectures on network systems. CreateSpace, 2018, vol. 1.
- [50] R. Sepulchre, M. Jankovic, and P. V. Kokotovic, Constructive nonlinear control. Springer Science & Business Media, 2012.